Control of Molecular Structures and Photophysical Properties of Zinc(II) Porphyrin Dendrimers Using Bidentate Guests: Utilization of Flexible Dendrimer Structures as a Controllable Mold

Jaesung Yang,[†] Sung Cho,[†] Hyejin Yoo,[†] Jaehong Park,[†] Wei-Shi Li,[‡] Takuzo Aida,*[,‡,§] and Dongho Kim*[,†]

Center for Ultrafast Optical Characteristics Control and Department of Chemistry, Yonsei University, Seoul 120-749, Korea, ERATO-SORST Nanospace Project, Japan Science and Technology Agency (JST), National Museum of Emerging Science and Innovation, 2-41 Aomi, Koto-ku, Tokyo 135-0064, Japan, and Department of Chemistry and Biotechnology, School of Engineering, and Center for NanoBio Integration, The University of Tokyo, 7-3-1 Hongo, Bunkyo-ku, Tokyo 113-8656, Japan

We have prepared supramolecular assemblies of hexaaryl-anchored polyester zinc(II) porphyrin dendrimers (**6P$_{Zn}$W**, **12P$_{Zn}$W**, and **24P$_{Zn}$W**) with various bipyridyl guests (**C$_n$Py$_2$**; n = 1, 2, 4, 6, and 8) through self-assembled coordination to control the structures and photophysical properties. We comparatively investigated the photophysical properties of porphyrin dendrimers with and without guest binding by using ensemble and single-molecule spectroscopy. The spectrophotometric titration data of dendrimers with guest molecules provide a strong indication of the selective intercalation of bipyridyl guests into porphyrin dendrimers. The representative dendrimer assembly **12P$_{Zn}$W⊃C$_6$Py$_2$** exhibits increased fluorescence quantum yield and lifetime in ensemble measurements, as well as higher initial photon count rates with stepwise photobleaching behavior in the single-molecule fluorescence intensity trajectories (FITs) compared to **12P$_{Zn}$W**. At the single-molecule level, the higher photostability of **12P$_{Zn}$W⊃C$_6$Py$_2$** can be deduced from the long durations of the first emissive levels in the FITs. We attribute the change in photophysical properties of the dendrimer assemblies to their structural changes upon intercalation of guest molecules between porphyrin units. These results provide new insight into the control of porphyrin dendritic structures using appropriate bidentate guests in poor environmental conditions.

Introduction

Dendrimers are intriguing step-growth polymers consisting of three parts: a central core, an interior dendritic structure, and an exterior surface. The dendrimer structure is easily controlled because each level of synthesis is normally carried out by a repetitive sequence of steps leading to more soluble and relatively less viscous structures compared to linear polymers.[1] Moreover, supramolecular assemblies can be constructed by incorporating guest molecules inside the interior branches of dendrimers.[2] As a strategy for the preparation of artificial light-harvesting systems, multichromophore dendrimer composites have been envisaged.[3–9] The combination of the high light-absorption capabilities of porphyrins and the 3D extended geometry of porphyrin dendrimers provides a good choice for mimicking the natural light-harvesting apparatus. In particular, the rigid hexaaryl-anchored polyester zinc(II) porphyrin dendrimers display a well-ordered 3D structure and rapid 3D energy migration processes among the constituent porphyrin units.[10]

For porphyrin dendrimers to be realized in highly efficient photonic devices, it is crucial to maintain the well-ordered uniform 3D structures to exhibit the desired properties in any given local environment or a small change of local environment. Unfortunately, however, the structures and photophysical prop-

erties of hexaaryl-anchored polyester zinc(II) porphyrin dendrimers are not maintained in poor solvents and polymer matrixes because of the solvophobic effect and the absence of a solvation medium, respectively. This unfavorable solvation is caused by the intrinsic flexibility of the interior branches of dendrimers: flexible repeat units and empty volumes between repeat branches.[11] To overcome the heterogeneities of dendrimers caused by different local environments, we have prepared supramolecular assemblies of hexaaryl-anchored polyester zinc(II) porphyrin dendrimers (**6P$_{Zn}$W**, **12P$_{Zn}$W**, and **24P$_{Zn}$W**) with various bipyridyl guests (**C$_n$Py$_2$**; n = 1, 2, 4, 6, and 8) through self-assembled coordination between the central metal atoms of zinc(II) porphyrins and the pyridyl ends of the guest molecules (Chart 1).

To explore the manipulation of dendrimer structures using bidentate guests, we carried out a steady-state spectrophotometric titration between zinc(II) porphyrin dendrimers and bipyridyl guests, time-resolved fluorescence decay measurements, and single-molecule fluorescence intensity trajectory measurements in chloroform and the solid phase. Consequently, we could control the dendrimer structures and their photophysical properties using specific bidentate guests and propose a new method for maintaining the intrinsic dendrimer character, even in solid phase. Moreover, the association patterns of porphyrin dendrimers with bidentate guests can be a good chemical ruler for estimating the interchromophore distance and vacant volume between the constituent porphyrin units and comparing the similarity of dendrimer geometries. Porphyrin dendrimers

---

* To whom correspondence should be addressed. E-mail: dongho@yonsei.ac.kr (D.K.), aida@macro.t.u-tokyo.ac.jp (T.A.).
[†] Yonsei University.
[‡] Japan Science and Technology Agency (JST).
[§] The University of Tokyo.

CHART 1: Molecular Structures of Hexaaryl Benzene Anchored Zinc(II) Porphyrin Dendrimers (6P$_{Zn}$W, 12P$_{Zn}$W, and 24P$_{Zn}$W), Dendrons (1P$_{Zn}$ and 2P$_{Zn}$), and Bipyridyl Derivative Guests (C$_n$Py$_2$; n = 1, 2, 4, 6, and 8)
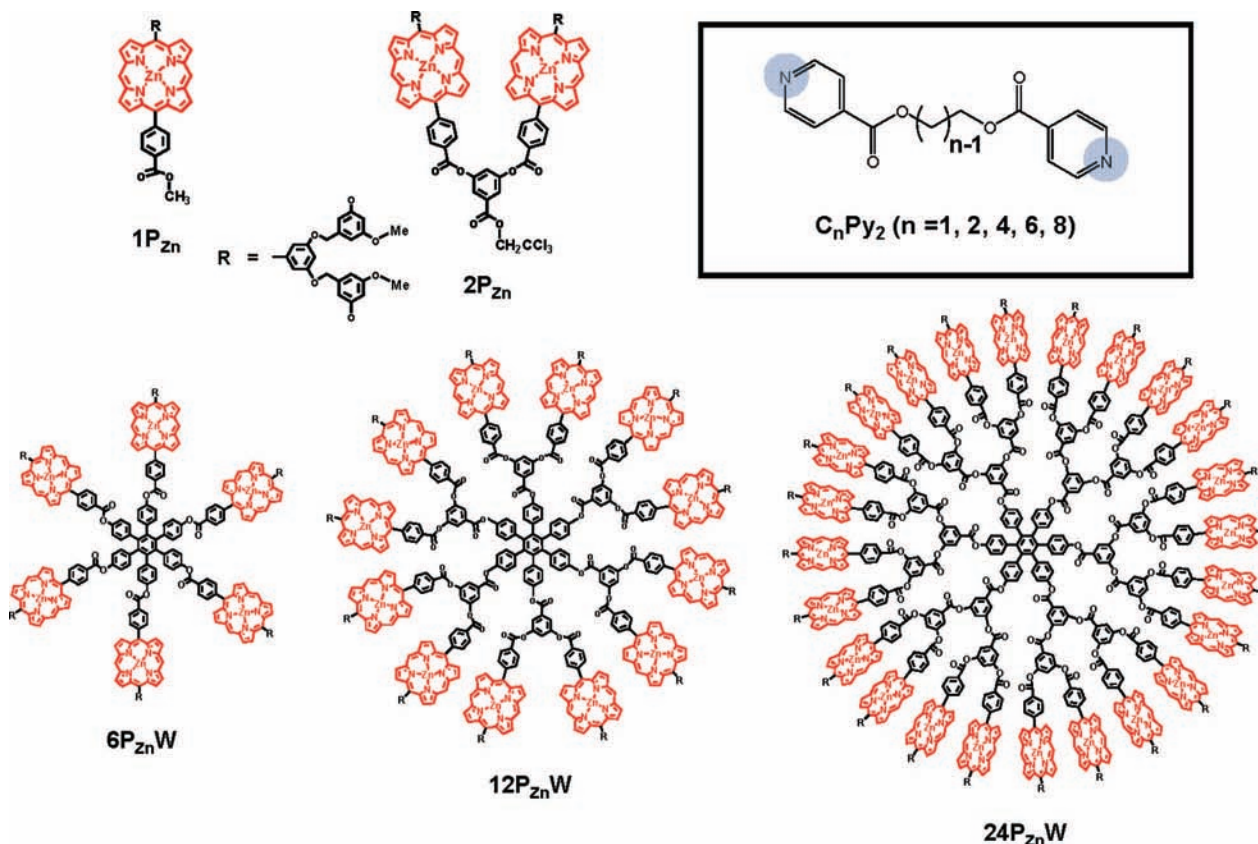
intercalated by bipyridyl guests show improved photostability and fluorescence quantum efficiency, which suggests that the supramolecular dendrimer assemblies can be a good candidate for light-harvesting photonic devices in the solid phase.

Experimental Methods

Sample Preparation. The zinc(II) porphyrin dendrimers and dendrons were synthesized according to a previously reported method[2] and dissolved in chloroform solvent (Sigma-Aldrich, spectrophotometric grade). All measurements were performed at ambient temperature (22 ± 1 °C). Samples for single-molecule measurements were prepared by spin-coating solutions of **12P$_{Zn}$W** and **12P$_{Zn}$W⊃C$_6$Py$_2$** (3 × 10^{-10} M) in chloroform containing 10 mg/mL poly(methyl methacrylate) (PMMA) polymer matrix (Sigma-Aldrich, average molecular weight = 120 000) onto rigorously cleaned coverslips at 2000 rpm.

Ensemble Spectroscopy. Steady-state absorption spectra were obtained with a UV−vis spectrometer (Varian, model Cary5000), and steady-state fluorescence was measured with a fluorometer (Hitachi, model F-2500). The fluorescence quantum yield was obtained in comparison to the fluorescence quantum yield of ∼0.03 of a zinc(II) 5,15-diphenylporphine at ambient temperature (22 ± 1 °C). A time-correlated single-photon-counting (TCSPC) system was used to measure spontaneous fluorescence decay. The system consisted of a cavity-dumped Kerr lens mode-locked Ti:sapphire laser pumped by a continuous-wave (CW) Nd:YVO$_4$ laser (Coherent, Verdi). The full width at half-maximum (fwhm) of the instrument response function (IRF) obtained for a dilute solution of coffee cream was typically 70 ps in our TCSPC system. The fluorescence decays were measured with magic-angle (54.7°) fluorescence polarization, and the number of fluorescence photons per unit time, detected by a photomultiplier tube, was always

maintained to <1% of the repetition rate of the excitation pulses, to prevent pileup distortion in the decay profiles. The intensity of the excitation pulses was carefully controlled by a variable neutral density (ND) filter to prevent multiphoton processes such as singlet−singlet annihilation.

Single-Molecule Spectroscopy. Fluorescence intensity trajectories of single molecules were obtained using a homemade confocal microscope with a microscope objective lens (Plan-neofluar x100 oil immersion, Carl Zeiss) and an avalanche photodiode (SPCM-AQR-13-FC, EG&G, PerkinElmer Optoelectronics, Norwalk, CT). A detailed description of the confocal microscope used in this work is presented elsewhere.[12] Briefly, an excitation laser beam of 543.5 nm from a He−Ne laser (25 LGR 193-230, Melles Griot) with an irradiation power of 0.5 µW was reflected onto the sample through a microscope objective lens by a dichroic beam splitter (565DCXR, Chroma). Fluorescence of single molecules was collected with a binning time of 30 ms by the same objective lens and focused onto an avalanche photodiode (APD) detector through suitable filters to reduce scattered excitation light. To suppress fast photobleaching of the samples by singlet oxygen, single-molecule detection was performed under oxygen-depleted environment obtained with flowing N$_2$.

Results

Selective Bidentate Guest Intercalation into Porphyrin Dendrimers. A series of absorption spectra of zinc(II) porphyrin dendrimers and dendrons in chloroform displayed in Figure 1a show largely perturbed B bands near 410 nm.

In particular, **12P$_{Zn}$W** exhibits a slightly blue-shifted, broad B band with a shoulder at 400 nm. However, the Q bands of the porphyrin dendrimers and dendrons are nearly the same as that of monomer. In accordance with the perturbed absorption
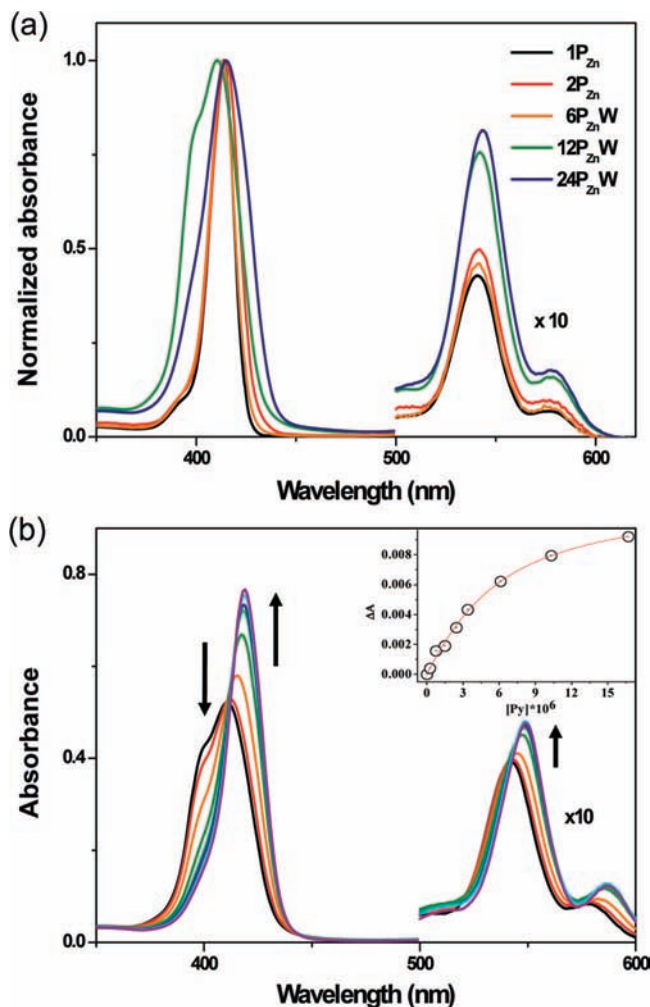
Zinc(II) Porphyrin Dendrimers

J. Phys. Chem. A, Vol. 112, No. 30, 2008 **6871**

Figure 1. (a) Steady-state absorption spectra of zinc(II) porphyrin dendrimers ($6P_{Zn}W$, $12P_{Zn}W$, and $24P_{Zn}W$) and dendrons ($1P_{Zn}$ and $2P_{Zn}$) in chloroform and (b) spectroscopic titration spectra of $12P_{Zn}W$ with C_6Py_2 ($0 \rightarrow 300$ equiv). The inset shows the absorbance change as the guest concentration increases and the fitted line as an association constant equation. A $12P_{Zn}W$ concentration of 2.90×10^{-9} M and a monitoring wavelength of 419 nm were used for the titration experiments. [Py] is the total number of binding sites of C_6Py_2, which was calculated as 2 times the concentration of C_6Py_2.

spectra, the fluorescence intensities of the porphyrin dendrimers are largely reduced in chloroform, whereas the absorption and fluorescence spectra of the porphyrin dendrimers in tetrahydrofuran are similar to those of the dendrons and the fluorescence quantum yields of the porphyrin dendrimers are maintained.[10] Accordingly, we can expect that the local environment of the porphyrin dendrimers in chloroform is unfavorable and that the structures of porphyrin dendrimers presumably collapse. The decreased distance between porphyrin units gives rise to stronger interchromophoric interactions in chloroform. However, chloroform does not affect the intrinsic properties of the constituent porphyrin units because of the rigid structure of porphyrin.

To overcome the environment dependence of the dendrimer structures and photophysical properties, we prepared five bipyridyl guests with various interpyridyl distances (Chart 1). As the concentration of the bipyridyl guest C_6Py_2 increases, the B band observed in the absorption spectra of $12P_{Zn}W$ becomes narrower, and the blue shoulder is removed, as shown in Figure 1b. From the spectrophotometric titration data of zinc(II) porphyrin dendrimers with bipyridyl guests, we obtained an association constant (K_{assoc}) that represents the degree of

complexation between porphyrin dendrimers and guests. The K_{assoc} values of the porphyrin dendrimers obviously show that the bipyridyl guests act as bidentate ligands with two binding sites because the association constants of the porphyrin dendrimers with C_nPy_2 ($n = 1, 2, 4, 6,$ and 8) are at least 2 orders of magnitude larger than that with pyridine (monodentate ligand). The narrow B band of the porphyrin dendrimers indicates a homogeneous local environment and reduced interchromophoric interactions between the constituent porphyrin units through anchoring of the porphyrin moieties by the bidentate guests.

The K_{assoc} values between the porphyrin dendrimers and bidentate guests with various interpyridyl distances largely depend on the 3D dendrimer structure: the interchromophore distance, the size of the vacant volume between porphyrin units, and the chain length between the two pyridyl groups. Figure 2 shows the K_{assoc} value patterns as a function of chain length between the two pyridyl units.

The K_{assoc} value of dendron $2P_{Zn}$ gradually increases as the length of the bipyridyl guests increases, as the two porphyrin units in $2P_{Zn}$ are located farthest away due to a lack of steric congestion. On the other hand, the K_{assoc} values of $6P_{Zn}W$ show a zigzagged pattern from which the selective intercalation of the bipyridyl guests can be deduced. C_1Py_2 and C_6Py_2 are the most effective bidentate guests to make supramolecular assemblies with $6P_{Zn}W$. Interestingly, $12P_{Zn}W$ shows a K_{assoc} pattern similar to that of $6P_{Zn}W$ because of the similarity in the optimized structures in that $6P_{Zn}W$ is a hexagonal wheel structure and $12P_{Zn}W$ is a staggered dual hexagonal wheel structure.[10] The long bipyridyl guests are expected to principally bind two porphyrin units in neighboring dendron units to restore the dual hexagonal wheel structure. It should be noted that $6P_{Zn}W$ shows a higher selectivity to the guest than $12P_{Zn}W$ because of its rigid structure, as $6P_{Zn}W$ is constructed using only one repeat unit between the hexaaryl benzene core and the porphyrin unit. The K_{assoc} pattern of $24P_{Zn}W$ with guests is also similar to those of the other porphyrin dendrimers. However, the long guests, C_6Py_2 and C_8Py_2, show significantly increased K_{assoc} values. We attribute this feature to the fact that, because the porphyrin units in $24P_{Zn}W$ are densely packed and the long bipyridyl guests are flexible, C_6Py_2 and C_8Py_2 can bind between certain suitable porphyrin units that might be not restricted between neighboring units. Furthermore, the flexible structure of $24P_{Zn}W$ enables it to change its local morphology to readily adapt to bidentate guests. Therefore, the K_{assoc} value patterns for guests of various lengths can serve as a chemical indicator for estimating the interchromophore distance, as well as a gauge for comparing the similarity of the 3D dendrimer structures.

Figure 3 shows the fluorescence decay profiles of zinc(II) porphyrin dendrimers coordinated with bidentate guests and pyridine as a reference in chloroform.

$6P_{Zn}W$ exhibits a fluorescence quantum yield similar to that of monomer ($\Phi_{F,monomer} = 0.03$) but a reduced S_1 fluorescence lifetime because of an additional fast decay component with a 400-ps time constant. The S_1 fluorescence lifetimes of the porphyrin dendrimers become shorter as the number of porphyrin units increases (Table 1).

The reduced S_1 fluorescence lifetimes of the dendrimers are coincident with reduced fluorescence quantum yields. In a good solvent, the constituent porphyrin units of the dendrimer are located at the farthest point in 3D space to minimize steric congestion. On the other hand, because the porphyrin dendrimer in a poor solvent is too flexible to maintain a well-ordered 3D
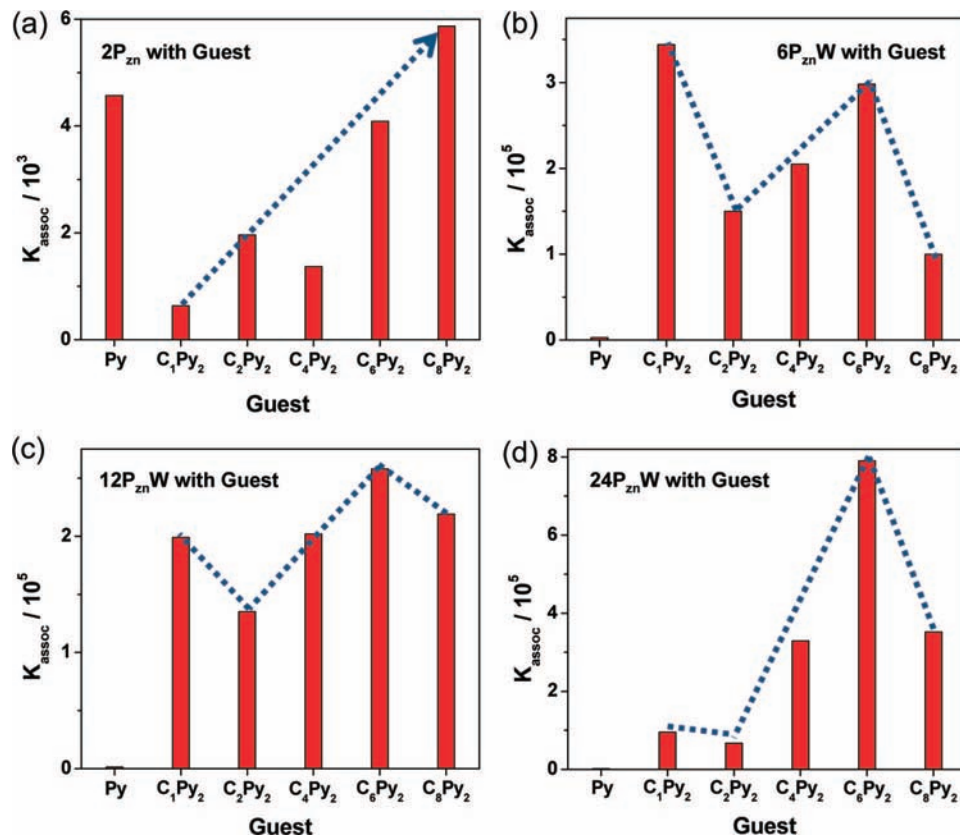
Figure 2. Association constant (K_{assoc}) pattern spectra of (a) **2P$_{Zn}$**, (b) **6P$_{Zn}$W**, (c) **12P$_{Zn}$W**, and (d) **24P$_{Zn}$W** with pyridine and bipyridyl guests (**C$_n$Py$_2$**; n = 1, 2, 4, 6, and 8) in chloroform. Dotted lines show characteristic binding patterns in each spectrum as the chain length between the two pyridyl groups of the bipyridyl guests increases.

structure, the overall 3D structure collapses and aggregates to minimize the contact area in the poor solvent environment. Consequently, **12P$_{Zn}$W** and **24P$_{Zn}$W**, consisting of two and three repeat units with 12 and 24 porphyrin units, respectively, are strongly affected and exhibit fluorescence lifetimes that are 1.5 and 1.7 times shorter than that of **6P$_{Zn}$W** because the aggregated state is normally nonemissive, leading to a reduction in the fluorescence lifetimes and quantum yields mainly as a result of enhanced $\pi-\pi$ stacking interactions between the constituent porphyrin moieties.

Single-Molecule Fluorescence Intensity Trajectories in PMMA Matrix. To obtain in-depth information on the guest binding effect, we measured the fluorescence intensity trajectories (FITs) of single dendrimer molecules embedded in a PMMA polymer matrix. We chose **12P$_{Zn}$W⊃C$_6$Py$_2$** as a representative dendrimer assembly and **12P$_{Zn}$W** as a reference compound, for which typical FITs are presented in Figure 4.

Unfortunately, the dendrimer assemblies consisting of **24P$_{Zn}$W** and long guests, which showed the most remarkable guest binding effect, were excluded in the single-molecule experiments because of their intrinsically low fluorescence quantum yields resulting from their more flexible structures compared to that of **12P$_{Zn}$W** (Table 1).

The FIT for **12P$_{Zn}$W** shows repetitive intensity jumps to lower intensity levels and back to the initial intensity level, whereas that for **12P$_{Zn}$W⊃C$_6$Py$_2$** does not show such behavior within the first emissive level. Instead, it shows higher initial fluorescence counts and a stepwise photobleaching process except for collective on/off behaviors around 38 s. We compared the frequency of the reversible intensity jumps within the first emissive levels of **12P$_{Zn}$W** and **12P$_{Zn}$W⊃C$_6$Py$_2$** for 80 molecules. It is assumed that, at the first emissive level, the

structural difference is the major factor causing a difference in the frequency of reversible intensity jumps between **12P$_{Zn}$W** and **12P$_{Zn}$W⊃C$_6$Py$_2$** because all of the other conditions except for the addition of guest molecules are identical. In the other emissive levels, factors aside from structural differences such as photobleached chromophores acting as an excitation trap can also induce intensity jumps to lower or background intensity level. Accordingly, only the intensity jumps within the first emissive level should be considered for this analysis. About 47% of the FITs for **12P$_{Zn}$W** show reversible intensity jumps within the first emissive level, whereas only 20% of the FITs for **12P$_{Zn}$W⊃C$_6$Py$_2$** show such behavior.

Distribution of Initial Photon Count Rates and Durations. Figure 5a shows superimposed distributions of initial photon counts per binning time of 30 ms from 102 molecules of each **12P$_{Zn}$W** and **12P$_{Zn}$W⊃C$_6$Py$_2$**.

The distribution for **12P$_{Zn}$W⊃C$_6$Py$_2$** becomes broad and is slightly shifted to higher count rate together with a significant reduction at low count rates compared to that for **12P$_{Zn}$W**. Perhaps the broad distribution is due to various constructs through the intercalation of guest molecules into the porphyrin dendrimer. The majority of the dendrimers probably show that some constituent porphyrin units forming aggregates are isolated through coordination with the guest molecules but others remain as aggregates within the porphyrin dendrimer. It is also noteworthy that the distribution for **12P$_{Zn}$W⊃C$_6$Py$_2$** is extended to higher count rates above 150 counts per 30 ms compared to that for **12P$_{Zn}$W** (inset of Figure 5a). Interestingly, all of the FITs of molecules showing such behavior exhibit single-step photobleaching or stepwise photobleaching with little off-times.

In the FITs of single molecules, the first emissive level can be regarded as reflecting the intact status of molecules prior to
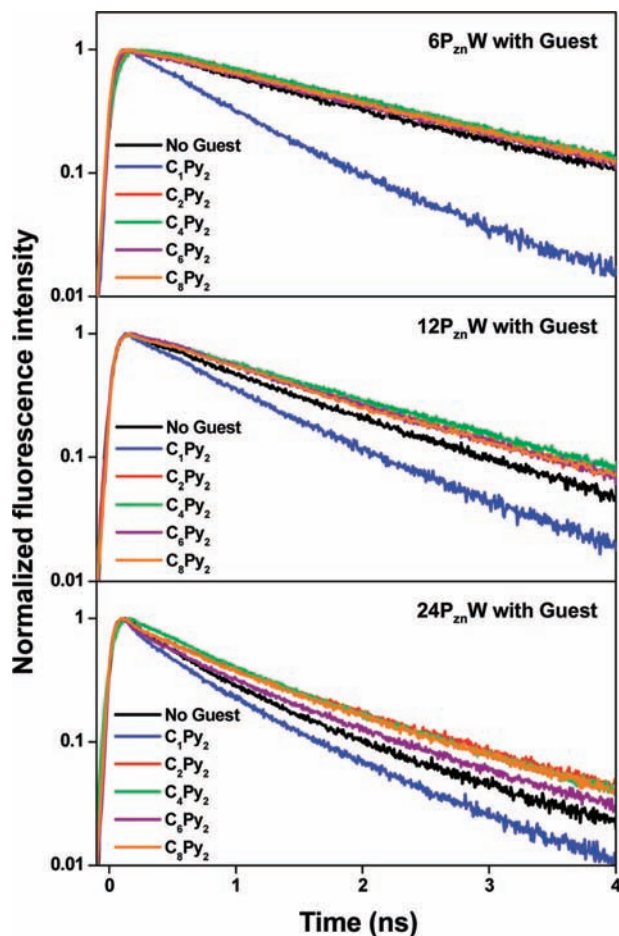
Zinc(II) Porphyrin Dendrimers

J. Phys. Chem. A, Vol. 112, No. 30, 2008 **6873**

Figure 3. Fluorescence decay profiles of zinc(II) porphyrin dendrimers ($6P_{Zn}W$, $12P_{Zn}W$, and $24P_{Zn}W$) with bipyridyl guests (C_nPy_2; $n = 1$, 2, 4, 6, and 8) in chloroform observed at 660 nm after photoexcitation of 405 nm. A molar ratio of 1:1 between the number of binding sites in the dendrimers and the number of binding sites in the bipyridyl guests was used. See Table 1 for details.

Figure 4. Representative fluorescence intensity trajectories of (a) $12P_{Zn}W$ and (b) $12P_{Zn}W \supset C_6Py_2$ embedded in PMMA under an oxygen-depleted environment obtained with flowing N_2.

transformation by photoexcitation. Accordingly, a long duration for the first emissive level can be strongly correlated with the photostability of the overall molecular system. Figure 5b shows superimposed distributions of the durations of the first emissive levels for $12P_{Zn}W$ and $12P_{Zn}W \supset C_6Py_2$. The distribution for $12P_{Zn}W \supset C_6Py_2$ is shifted to longer durations than that for $12P_{Zn}W$, with average durations of 3.4 and 5.8 s for $12P_{Zn}W$ and $12P_{Zn}W \supset C_6Py_2$, respectively. This feature indicates that the intercalation of bidentate guest C_6Py_2 into $12P_{Zn}W$ reduces the possibility of photoinduced transformation by 41%. However, the overall survival times of $12P_{Zn}W$ and $12P_{Zn}W \supset C_6Py_2$ in the FITs are similar at 25 and 28 s, with standard deviations of 23 and 24 s, respectively. This tendency in the total survival times is probably due to the fact that a dominant factor contributing to the overall survival time in the FITs is the total number of chromophores in weakly interacting multichromophoric systems.[13]

Discussion

Bidentate Guest Binding. Bidentate guests can affect the structures and photophysical properties of porphyrin dendrimers because the bidentate guest intercalated between porphyrin units acts as a spacer to elongate the interchromophore distance and interrupt aggregation. In addition, the relative orientation between porphyrin units in the dendrimer is also controlled by
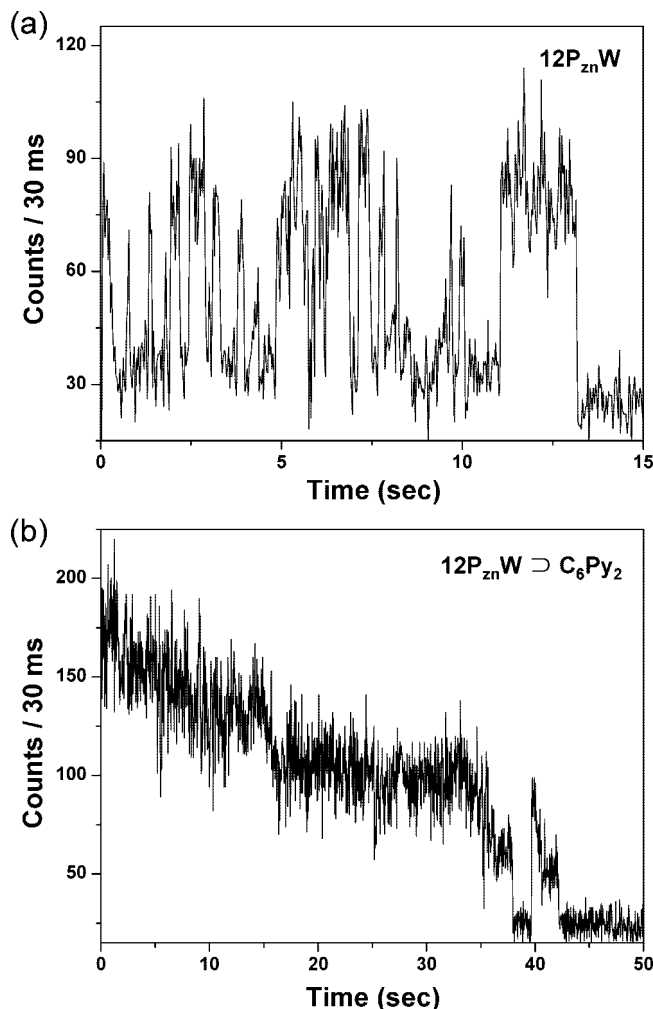
the binding of the guest. For example, C_1Py_2, the shortest guest, reduces the interchromophore distance and makes only a coplanar geometry between porphyrin units because of the short interpyridyl distance. In particular, $6P_{Zn}W$ is strongly affected by C_1Py_2, having a much reduced fluorescence quantum yield and lifetime. The interchromophore distance between the porphyrin units of $6P_{Zn}W$ based on a geometry-optimized quantum calculation is 16.9 Å, but the interpyridyl distance is only 10.2 Å. Accordingly, C_1Py_2 induces a stronger interchromophore interaction between porphyrin units and makes a gable geometry. Consequently, the shortest bidentate guest increases interchromophoric interactions, leading to accelerated nonradiative decay processes.

On the other hand, the other guests increase the portion of the slow component in the S_1 fluorescence decay and the fluorescence quantum yield of the porphyrin dendrimers. $6P_{Zn}W$ is not affected by the longer guests because the intercalated bipyridyl guests are too flexible to change the molecular structure of $6P_{Zn}W$, which has only one repeat unit between the hexaaryl benzene core and the porphyrin unit. In contrast, $12P_{Zn}W$ and $24P_{Zn}W$, which exhibit flexible conformations because of their increased numbers of repeat units, show significantly longer S_1 fluorescence lifetimes and larger fluorescence quantum yields. For example, the complexes of $12P_{Zn}W$ and $24P_{Zn}W$ with C_6Py_2 have fluorescence quantum yields that increase by 54% and 50%, respectively, and the

TABLE 1: Relative Fluorescence Quantum Yields (Φ_F) and Fitted S_1 State Fluorescence Lifetimes (τ_F) of Zinc(II) Porphyrin Dendrimers ($6P_{Zn}W$, $12P_{Zn}W$, and $24P_{Zn}W$) with Bipyridyl Guests (C_nPy_2; $n = 1, 2, 4, 6$, and 8) and Pyridine in Chloroform[a]

	$6P_{Zn}W$		$12P_{Zn}W$		$24P_{Zn}W$	
	Φ_F	τ_F (ns)[b]	Φ_F	τ_F (ns)	Φ_F	τ_F (ns)
no guest	0.030	0.39 (34.2)[c] 1.85 (65.8)	0.016	0.05 (35.0) 0.47 (26.5) 1.42 (38.5)	0.008	0.10 (47.8) 0.50 (37.5) 1.51 (14.7)
C_1Py_2	0.014	0.46 (54.3) 0.78 (41.0)	0.012	0.33 (44.6) 0.76 (51.6) 1.49 (3.7)	0.007	0.13 (38.4) 0.49 (45.7) 1.07 (15.9)
C_2Py_2	0.022	0.29 (11.6) 1.75 (88.4)	0.022	0.22 (24.9) 1.52 (75.1)	0.011	0.14 (38.4) 0.70 (28.3) 1.62 (33.3)
C_4Py_2	0.029	0.19 (15.3) 1.83 (84.7)	0.024	0.41 (19.1) 1.61 (80.9)	0.011	0.14 (44.9) 0.72 (36.9) 1.73 (18.2)
C_6Py_2	0.029	0.25 (17.5) 1.79 (82.5)	0.025	0.27 (26.1) 1.61 (73.9)	0.012	0.15 (41.0) 0.71 (37.0) 1.70 (22.0)
C_8Py_2	0.030	0.17 (22.3) 1.79 (77.7)	0.024	0.17 (22.7) 1.79 (77.3)	0.011	0.13 (30.8) 0.69 (30.3) 1.60 (38.9)
pyridine	0.030		0.015		0.008	

[a] Molar ratio of 1:1 between the number of binding sites in the dendrimers and the number of binding sites in the bipyridyl guests was used for all experiments. [b] Fluorescence decays were obtained by applying an excitation wavelength of 550 nm. [c] Values in parentheses are the relative amplitudes of each time constant.

corresponding average S_1 fluorescence lifetimes become 1.8 and 1.5 times longer, compared to the values for their uncoordinated dendrimers. We attribute this difference to isolation of the constituent porphyrin units by the intercalated guest molecules, leading them to act as an individual monomers. Accordingly, the longer bidentate guests (C_nPy_2, $n = 4, 6, 8$) are a good choice for controlling the interchromophore interactions in large dendrimers such as $12P_{Zn}W$ and $24P_{Zn}W$.

Bidentate Guest Binding Effects Probed by Single-Molecule Fluorescence Detection. The FITs of $12P_{Zn}W \supset C_6Py_2$ show stepwise photobleaching and a low occurrence of intensity jumps. We reported previously that such behaviors are observed in multichromophoric systems in which the interactions between neighboring chromophores are so weak that each chromophore acts as an individual absorbing and emitting unit. In such systems, the energetically lowest chromophoric site behaves as an excitation energy trapping site and is responsible for fluorescence, in combination with the temporal evolution of the trapping site due to photobleaching.[12–17] Accordingly, the intercalation of guest molecules can lead to the isolation of strongly interacting constituent porphyrin units to show individual characters within the dendrimer.

Because the absorption cross section of $12P_{Zn}W \supset C_6Py_2$ is similar to that of $12P_{Zn}W$ at the excitation wavelength, a competition between fluorescence from the singlet excited state and nonradiative relaxation processes mainly contributes to the photon counts in the FITs.[13] In this regard, by comparing the initial photon count rates between $12P_{Zn}W$ and $12P_{Zn}W \supset C_6Py_2$, we can estimate the extent of nonradiative decay channels acting as fluorescence quenching sites intrinsically residing in the porphyrin dendrimer. The average initial photon count rates for $12P_{Zn}W$ and $12P_{Zn}W \supset C_6Py_2$ are 1570 and 2150 counts·s^{-1}, respectively. The increase of approximately 37% in the initial photon count rate of $12P_{Zn}W \supset C_6Py_2$ indicates that the extent of nonradiative decay channels for

excitation energy relaxation processes is presumably reduced through the intercalation of the guest molecules. We can verify from these results that the coordination between the central zinc metal atoms and the pyridyl end groups of the guest molecules is strong enough even in a poor environment, the solid phase, to control the structure of the porphyrin dendrimer wheel.

Photostability of Porphyrin Dendrimer Wheel. The ability of porphyrin dendrimers to maintain an intact status against repetitive photoexcitation is increased as the guest molecules are intercalated between constituent porphyrin units. One of the possible explanations for this behavior is that aggregates in $12P_{Zn}W$ give rise to photoinduced intramolecular charge transfer. The small porphyrin ring separation in the collapsed structure of $12P_{Zn}W$ causes a significant orbital overlap between the constituent porphyrin units to result in ring-to-ring charge transfer (RRCT). When $12P_{Zn}W$ is excited to the lowest singlet excited state, electron transfer between porphyrin units likely proceeds via a triplet excited state to form a triplet radical pair, as the triplet quantum yield of metalloporphyrin is relatively high and the experiment was performed under N_2 flowing to remove oxygen. Photoinduced RRCT is frequently observed for cofacial diporphyrins or metal−porphyrin sandwich complexes in which porphyrin macrocycles are separated by approximately 3 Å.[18–20] Hence, the decreased probability of radical pair formation via RRCT through the coordination of guest molecules to isolate aggregated porphyrin moieties is probably responsible for the increased photostability of $12P_{Zn}W \supset C_6Py_2$.

It should be noted that the lower frequency of reversible intensity jumps within the first emissive level in the FITs of $12P_{Zn}W \supset C_6Py_2$ can also be explained by a similar mechanism. Recently, some articles reported that electron transfer between the molecules and the surrounding polymer matrix can be associated with long off-times with average times of several seconds.[21–24] Because most of the reversible intensity jumps of porphyrin dendrimers occur to lower intensity levels than the
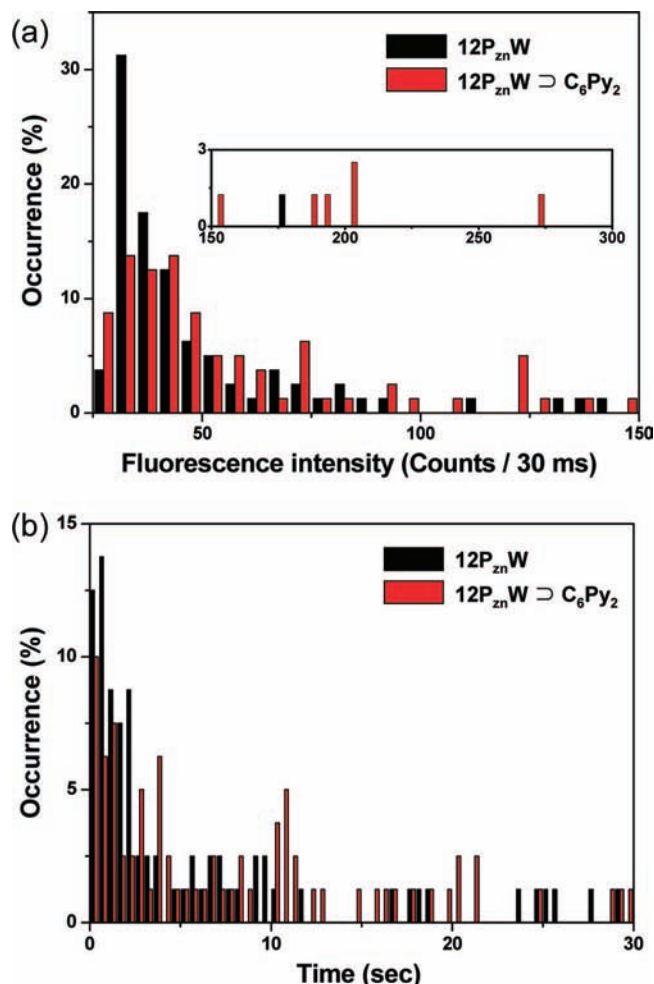
Zinc(II) Porphyrin Dendrimers

J. Phys. Chem. A, Vol. 112, No. 30, 2008 **6875**

Figure 5. Distributions for (a) fluorescence intensity and (b) duration of the first emissive levels of **12P$_{Zn}$W** and **12P$_{Zn}$W⊃C$_6$Py$_2$** embedded in PMMA under an oxygen-depleted environment obtained with flowing N$_2$. The inset in a is the same distribution at higher count rates. Both distributions were constructed from 102 single molecules of either **12P$_{Zn}$W** or **12P$_{Zn}$W⊃C$_6$Py$_2$**. The *y* axis in each distribution gives the relative occurence as a percentage.

background intensity level with a time scale of several hundreds of milliseconds, it is difficult to relate the spurious electron transfer with more frequent reversible intensity jumps in the collapsed structure of **12P$_{Zn}$W**. Thus, the difference in the frequency of reversible intensity jumps between **12P$_{Zn}$W** and **12P$_{Zn}$W⊃C$_6$Py$_2$** can be ascribed to intramolecular electron transfer between constituent porphyrin units upon photoexcitation. The relaxation of the collapsed structure by the coordination of guest molecules with **12P$_{Zn}$W** can account for the low frequency of reversible intensity jumps within the first emissive level of the FITs for **12P$_{Zn}$W⊃C$_6$Py$_2$**.

Another possible explanation for the increased photostability of **12P$_{Zn}$W⊃C$_6$Py$_2$** could be that the heat released when the photoexcited molecules relax to the ground state through nonradiative decay processes can increase the probability of thermal deformation of the molecules. Thus, the decreased nonradiative decay pathways in **12P$_{Zn}$W⊃C$_6$Py$_2$** as a result of the relaxation of collapsed structure might increase the photo-stability of the porphyrin dendrimers.

Conclusions

Flexible dendrimers are well-suited for the construction of supramolecular assemblies by an appropriate choice of guest

molecules. Depending on the chain length between the two pyridyl ends of the guest molecule, porphyrin dendrimers exhibit the efficient formation of self-assembled constructs between porphyrin units and guests along with a specific association pattern. In poor local environments, the porphyrin dendritic structures are not maintained, and their photophysical properties are also largely perturbed. Our ensemble and single-molecule spectroscopic data on supramolecular dendrimer assemblies illustrate that the structures and photophysical properties of porphyrin dendrimers can be controlled by the intercalation of bidentate guests between constituent porphyrin units and that the guest binding effect is maintained even in the solid phase. In particular, **12P$_{Zn}$W** and **24P$_{Zn}$W** with longer bidentate guests show a tendency to restore the structure and photophysical properties of intact dendrimers in good solvents. In this context, we could suggest the required conditions for controlling the dendrimer properties such as structural rigidity and a proper chain length between the binding sites of guest molecules. Finally, based on our investigations, we believe that the guest controllable dendrimer assembly can be a good candidate for a solid-state photonic device.

References and Notes

(1) Stevens, M. P. *Polymer Chemistry*, 3rd ed.; Oxford University Press: New York, 1999; pp 301−303.

(2) (a) Li, W.-S.; Jiang, D.-L.; Suna, Y.; Aida, T. *J. Am. Chem. Soc.* **2005**, *127*, 7700. (b) Li, W.-S.; Kim, K. S.; Jiang, D.-L.; Tanaka, H.; Kawai, T.; Kwon, J. H.; Kim, D.; Aida, T. *J. Am. Chem. Soc.* **2006**, *128*, 10527.

(3) Kimble, M. *Femtochemistry VII: Fundamental Ultrafast Processes in Chemistry, Physics, and Biology*; Castleman, W., Jr., Ed.; Elsevier: Amsterdam, 2006; pp 113−116.

(4) Martin, M. M.; Hynes, J. T. *Femtochemistry and Femtobiology: Ultrafast Events in Molecular Science*; Elsevier: Amsterdam, 2004; pp 495−498.

(5) (a) Larsen, J.; Brüggemann, B.; Khoury, T.; Sly, J.; Crossley, M. J.; Sundström, V.; Åkesson, E. *J. Phys. Chem. A* **2007**, *111*, 10589. (b) Larsen, J.; Brüggemann, B.; Sly, J.; Crossley, M. J.; Sundström, V.; Åkesson, E. *Chem. Phys. Lett.* **2006**, *433*, 159. (c) Larsen, J.; Brüggemann, B.; Polivka, T.; Sundström, V.; Åkesson, E.; Sly, J.; Crossley, M. J. *J. Phys. Chem. A* **2005**, *109*, 10654. (d) Larsen, J.; Andersson, J.; Polivka, T.; Sly, J.; Crossley, M. J.; Sundström, V.; Åkesson, E. *Chem. Phys. Lett.* **2005**, *403*, 205.

(6) (a) Choi, M.-S.; Yamazaki, T.; Yamazaki, I.; Aida, T. *Angew. Chem., Int. Ed.* **2004**, *43*, 150. (b) Choi, M.-S.; Aida, T.; Yamazaki, T.; Yamazaki, I. *Chem. Eur. J.* **2002**, *8*, 2668. (c) Choi, M.-S.; Aida, T.; Luo, H.; Araki, Y.; Ito, O. *Angew. Chem., Int. Ed.* **2003**, *42*, 4060.

(7) Yeow, E. K. L.; Ghiggino, K. P.; Reek, J. N.; Crossley, M. J.; Bosman, A. W.; Schenning, A. P. H. J.; Meijer, E. W. *J. Phys. Chem. B* **2000**, *104*, 2596.

(8) (a) Varnavski, O. P.; Ostrowski, J. C.; Sukhomlinova, L.; Twieg, R. J.; Bazan, G. C.; Goodson, T., III *J. Am. Chem. Soc.* **2002**, *124*, 1736. (b) Tomalia, D. A.; Naylor, A. M.; Goddard, W. A., III *Angew. Chem., Int. Ed. Engl.* **1990**, *29*, 138.

(9) (a) Hofkens, J.; Latterini, L.; De Belder, G.; Gensch, T.; Maus, M.; Vosch, T.; Karni, Y.; Schweitzer, G.; De Schryver, F. C. *Chem. Phys. Lett.* **1999**, *304*, 1. (b) Maus, M.; De, R.; Lor, M.; Weil, T.; Mitra, S.; Wiesler, U.-M.; Herrmann, A.; Hofkens, J.; Vosch, T.; Mullen, K.; De Schryver, F. C. *J. Am. Chem. Soc.* **2001**, *123*, 7668.

(10) Cho, S.; Li, W.-S.; Yoon, M.-C.; Ahn, T. K.; Jiang, D.-L.; Kim, J.; Aida, T.; Kim, D. *Chem. Eur. J.* **2006**, *12*, 7576.

(11) De Backer, S.; Prinzie, Y.; Verheijen, W.; Smet, M.; Desmedt, K.; Dehaen, W.; De Schryver, F. C. *J. Phys. Chem. A* **1998**, *102*, 5451.

(12) (a) Park, M.; Cho, S.; Yoon, Z. S.; Aratani, N.; Osuka, A.; Kim, D. *J. Am. Chem. Soc.* **2005**, *127*, 15201. (b) Park, M.; Yoon, M.; Yoon, Z. S.; Hori, T.; Peng, X.; Aratani, N.; Hotta, J.; Uji-i, H.; Sliwa, M.; Hofkens, J.; Osuka, A.; Kim, D. *J. Am. Chem. Soc.* **2007**, *129*, 3539.

(13) Hofkens, J.; Maus, M.; Gensch, T.; Vosch, T.; Cotlet, M.; Köhn, F.; Herrmann, A.; Müllen, K.; De Schryver, F. C. *J. Am. Chem. Soc.* **2000**, *122*, 9278.

(14) Yeow, E. K. L.; Melnikov, S. M.; Bell, T. D. M.; De Schryver, F. C.; Hofkens, J. *J. Phys. Chem. A* **2006**, *110*, 1726.

(15) Bopp, M.; Jia, Y.; Li, L.; Cogdell, R. J.; Hochstrasser, R. M. *Proc. Natl. Acad. Sci. U.S.A.* **1997**, *94*, 10630.

(16) Vanden Bout, D. A.; Yip, W.-T.; Hu, D.; Fu, D.-K.; Swager, T. M.; Barbara, T. F. *Science* **1997**, *277*, 22.

(17) Becker, K.; Lupton, J. M. *J. Am. Chem. Soc.* **2006**, *128*, 6468.

(18) (a) Yan, X.; Holten, D. *J. Phys. Chem.* **1988**, *92*, 409. (b) Bilsel, O.; Rodriguez, J.; Holten, D. *J. Am. Chem. Soc.* **1990**, *112*, 4075. (c) Bilsel, O.; Rodriguez, J.; Milam, S. N.; Gorlin, P. A.; Girolami, G. S.; Suslick, K. S.; Holten, D. *J. Am. Chem. Soc.* **1992**, *114*, 6528.

(19) (a) Netzel, T. L.; Bergkamp, M. A.; Chang, C. K. *J. Am. Chem. Soc.* **1982**, *104*, 1952. (b) Fujita, I.; Fajer, J.; Chang, C. K.; Wang, C. B.; Bergkamp, M. A.; Netzel, T. L. *J. Phys. Chem.* **1982**, *86*, 3754.

(20) Petke, J. D.; Maggiora, G. M. *J. Chem. Phys.* **1986**, *84*, 3.

(21) Haase, M.; Hübner, C. G.; Reuther, E.; Herrmann, A.; Müllen, K.; Basché, Th. *J. Phys. Chem. B* **2004**, *108*, 10445.

(22) (a) Schuster, J.; Cichos, F.; von Borczyskowski, C. *Opt. Spectrosc.* **2005**, *98*, 778. (b) Schuster, J.; Cichos, F.; von Borczyskowski, C. *Appl. Phys. Lett.* **2005**, *87*, 051915.

(23) Zondervan, R.; Kulzer, F.; Orlinskii, A. B.; Orrit, M. *J. Phys. Chem. A* **2003**, *107*, 6770.

(24) Hoogenboom, J. P.; van Dijk, E. M. H. P.; Hernando, J.; van Hulst, N. F.; Garcia-Parajó, M. F. *Phys. Rev. Lett.* **2005**, *95*, 097401.